

## RESEARCH ARTICLE

# A SOM-based analysis of the drivers of the 2015–2017 Western Cape drought in South Africa

Romarc C. Odoulami<sup>1</sup>  | Piotr Wolski<sup>2</sup>  | Mark New<sup>1,3</sup> 

<sup>1</sup>African Climate and Development Initiative, University of Cape Town, Cape Town, South Africa

<sup>2</sup>Climate System Analysis Group, University of Cape Town, Cape Town, South Africa

<sup>3</sup>School of International Development, University of East Anglia, Norwich, NR4 7TJ, United Kingdom

## Correspondence

Romarc C. Odoulami, African Climate and Development Initiative, University of Cape Town, Cape Town, South Africa.  
Email: romarc.odoulami@uct.ac.za

## Funding information

AXA Research Fund; BNP Paribas Climate Foundation; Department of Science and Technology (South Africa); National Research Foundation (South Africa); Southern African Systems Analysis Centre

## Abstract

The multi-year (2015–2017) drought in the South West of the Western Cape (SWC) caused a severe water shortage in the summer of 2017–2018, with damaging impacts on the local and regional economy, and Cape Town being in the news one of the first major cities to potentially run out of water. Here, we assess the links between the rainfall deficits during the drought and (a) large scale circulation patterns, (b) moisture transport, and (c) convective available potential energy (CAPE). We used self-organising maps (SOM) analysis to classify daily ERA-interim 850 hPa geopotential height for the period 1979–2017 (March–October) into synoptic types. This allowed us to identify the dominant synoptic states over Southern Africa that influence the local climate in the area affected by the drought. The results show that (a) the frequency of nodes with rain-bearing circulation types decreased during the drought; (b) the amount of rain falling on days that did have rain-bearing circulation types was reduced, especially in the shoulder seasons (March–May and August–October); (c) the rainfall reduction was also associated with anomalously low moisture transport, and convective energy (CAPE), over SWC. These results add to the existing knowledge of drivers of the Cape Town drought, providing an understanding of underlying synoptic processes.

## KEYWORDS

Cape Town, circulation, day zero, drought, self-organizing maps, South Africa, synoptic drivers, winter rainfall

## 1 | INTRODUCTION

The South West of the Western Cape (SWC) Province in South Africa experienced a multi-year drought, spanning the years 2015, 2016, and 2017, which contributed to the most severe water shortage experienced by the Province in the last century (Botai *et al.*, 2017). The fear of running out of water—called “Day Zero” in the media—before the onset of the winter rainfall season of 2018 forced the City of Cape Town to impose severe restrictions on water usage, and to

implement emergency supply augmentation measures. The drought and the associated water crisis had large socio-economic impacts at national and local levels. The Western Cape Province contributes about 14% to the country's Gross Domestic Product and its agricultural sector, one of the most affected because of the high dependence on water for irrigation, reported losses estimated to 5.9 billion of South African Rand in the 2017–2018 season (Pienaar and Boonzaaier, 2018). The length (2015–2017) and severity of the drought has attracted public and media

This is an open access article under the terms of the Creative Commons Attribution License, which permits use, distribution and reproduction in any medium, provided the original work is properly cited.

© 2020 The Authors *International Journal of Climatology* published by John Wiley & Sons Ltd on behalf of Royal Meteorological Society.

interest about the likely causes of the drought, including the potential influence of anthropogenic climate change on drought occurrence, persistence, and likelihood over the region.

The SWC is characterized by a mediterranean climate and is part of the austral winter rainfall region of Southern Africa. During the summer months (DJF), the two subtropical anticyclones—South Atlantic and South Indian High—form strong subsidence and a persistent high-pressure field over the subcontinent, leading to dry and warm conditions over the SWC (Reason, 2017). The SWC receives most of its rainfall, about 60–70%, during the winter months (June–August or JJA) (Reason and Jagadheesha, 2005), when the two subtropical anticyclones move northwards, enabling the strengthening and the northward expansion of the westerlies, and resulting in the rain-bearing frontal systems associated with mid-latitude cyclones moving across the SWC. Given the dominance of that mechanism, the variability of winter rainfall in the SWC depends on drivers affecting the position, strength, and frequency of these westerly cyclones.

The Antarctic Oscillation (AAO)—also called Southern Annular Mode (SAM)—which expresses pressure difference between mid- and low-latitudes, and thus indirectly influences the latitudinal position of the westerlies, has a strong influence on core winter rainfall over western South Africa. A negative AAO phase is correlated with wet JJA and is associated with: the northward shift of the subtropical jet, increases in low-level moisture transport, and increases in low-level convergence and vorticity, which overall indicate an equatorward shift and strengthening of the mid-latitude storm tracks in the vicinity of South Africa (Reason and Rouault, 2005). These relationships are reversed during positive AAO phases.

ENSO has a weaker influence on SWC rainfall. Philippon *et al.* (2012) reported a positive correlation between early winter (MJJ) rainfall over the Western Cape and the Niño3.4 index in the post-1976 period, but that relationship was not consistent through time, and not present in the other seasons, even in MAM and JAS. Other factors shown to affect SWC rainfall include local SST anomalies (Reason and Jagadheesha, 2005) and sea ice anomalies (Blamey and Reason, 2007).

While most of these studies focused on the relationship between specific synoptic drivers and rainfall variability in the Western Cape region, Wolski *et al.* (2018) used circulation classification with self-organizing maps (SOMs) to quantify rainfall variability that can be explained by the frequency of circulation types over a winter (Cape Town) and summer (Johannesburg) rainfall regime in South Africa. Over Cape Town, the synoptic states represented in the SOM classification of pressure field-related variables explained between 40 and 60% of

the winter (JJA) rainfall interannual variability at a local scale. Lennard and Hegerl (2015) examined the relationship between changes in synoptic-scale circulation and rainfall response under winter and summer rainfall regimes in South Africa using SOMs. They found that in the winter rainfall zone, mid-latitude cyclones are the dominant rain-bearing circulation states, and that there was a significant upward trend of summer (dry) circulation modes in summer, winter, and spring seasons over 31 years (1979–2009).

The synoptic anomalies underlying the 2015–2017 drought in the SWC have been described by Sousa *et al.* (2018) and Mahlalela *et al.* (2019). The first of those studies shows the strong influence of AAO (positive phase) and the associated poleward shift of moisture transport corridors (atmospheric rivers) due to the latitudinal expansion of the two subtropical high-pressure systems in the South Atlantic and Indian Oceans. The second study investigated the atmospheric mechanisms behind the drought with a major focus on the early winter (April–May) rainfall variability in the Southwestern Cape region, and found that dry early winters over the Southwestern Cape were associated with a stable atmosphere characterized by a weak subtropical jet and less moisture entering the region. Also, Burls *et al.* (2019) linked the drought to a long-term decrease in rainfall events during cold fronts over the Western Cape region. They associated these changes in rainfall characteristics to Hadley Cell expansion over the Southern Hemisphere and to the upward trend in high-pressure conditions in days following the passage of a frontal system. This process enhances drying particularly over the mountainous areas. Abba Omar and Abiodun (2020) investigated the characteristics of cut-off lows during the 2015–2017 Western Cape drought. Their findings suggest that an increased cut-off lows-related rainfall in 2015 and 2016 reduced the severity of the drought. But, in 2017, most cut-off lows were located further south and did not reach the Western Cape region, resulting in reduction of cut-off lows rainfall and increased severity of the drought.

Climate projections over Southern Africa indicate that the region will become drier, with significant expansions of arid and semi-arid zones due to global warming (Feng and Fu, 2013; Cook *et al.*, 2014; Niang *et al.*, 2014; Lehner *et al.*, 2017). The winter rainfall region in the southwest is also projected to experience drier conditions due to the southward shift of the mid-latitude rainfall producing systems (Moise and Hudson, 2008; Shongwe *et al.*, 2009; Department of Environmental Affairs, 2013). Consequently, people living in this region will become vulnerable to water scarcity and land degradation (Feng and Fu, 2013). Also, Lehner *et al.* (2017) and Niang *et al.* (2014) projected an increased risk of multi-year

severe droughts in these regions during the 21st century. Hence, the following question related to the nature and origin of the drought become relevant: Is the recent multi-year (2015–2017) drought in the SWC the “new normal” because of climate change? Otto *et al.* (2018) showed that the three year (2015–2017) precipitation mean, used to represent the meteorological aspects of the drought, was rare in the context of the last 100 years of data with probability of occurrence of 1 in 150 years (at a sub-regional scale; Wolski (2018) shows 1 in 300–400 years at local scale) and concluded that the likelihood of such drought has increased by a factor of three because of anthropogenic climate change. While that study provides essential information on the likelihood of the event and the contribution of anthropogenic climate change to its occurrence from the perspective of rainfall as a surface expression of the state of the climate system, it did not explicitly address the dynamical processes behind the 2015–2017 SWC drought. The present study contributes to addressing that gap.

This study identifies and characterizes the anomalies in atmospheric circulation as well as anomalies in rainfall responses to the synoptic forcing during the 2015–2017 SWC drought. We first apply the SOM algorithm to reanalysis datasets to identify the synoptic circulation states over Southern Africa and examine how they relate to rainfall characteristics over the SWC in South Africa during the 2015–2017 drought. In that, we extend studies by Sousa *et al.* (2018) and Mahlalela *et al.* (2019) by identifying the synoptic drivers of the 2015–2017 multi-year drought over the SWC using the SOM classification algorithm. Subsequently, we also analyse the relationship between the rainfall anomalies and the main meteorological variables describing the state of the local atmosphere. The following sections of this manuscript describe the data and methodology used in the study, present the main findings and discuss them in connection with previous studies.

## 2 | DATA AND METHODS

### 2.1 | Data

In this study, we used surface station observations and reanalysis datasets. The observational dataset comprises rainfall station records covering the SWC obtained from the South African Weather Service (SAWS). We quality-controlled the SAWS datasets and only used stations with less than 2.5% of missing daily data between January 1979 and October 2017. A total of 22 rainfall stations (Figure 1a) passed these quality criteria and were analysed in this study. The analysis includes all months between March and October from 1979 to 2017. We only

used the regional mean rainfall, calculated using the 22 selected stations in Figure 1a, except when otherwise specified. We also use a gridded rainfall dataset, the Global Precipitation Climatology Centre dataset (GPCC; Schneider *et al.*, 2011). GPCC provides global monthly precipitation available on different grid resolutions. For this study, we only analysed the GPCC monthly rainfall data at a grid resolution of  $1^\circ \times 1^\circ$  for the period 1979–2017 averaged over the SWC domain in Figure 1a ( $31\text{--}35^\circ\text{S}$  and  $17.5\text{--}21^\circ\text{E}$ )

To capture synoptic circulation over the region, we used the European Centre for Medium-Range Weather Forecasts (ECMWF) ERA-Interim (ERA-INT) reanalysis dataset (Dee *et al.*, 2011). ERA-INT data are available on the grid size of  $0.75^\circ \times 0.75^\circ$  from 1979 to 31 August 2019. The primary variable used to derive synoptic states is daily geopotential height at 850 hPa pressure level. We also used ERA-INT daily specific humidity ( $q$ ), meridional ( $v$ ) and zonal ( $u$ ) wind components ( $\vec{V}$ ) at all available pressure levels (from 1 to 1,000 hPa) to derive the daily moisture transport ( $Q$ ):

$$\vec{Q} = q \times \vec{V}, \quad (1)$$

We also analysed ERA-INT daily convective available potential energy (CAPE) and rainfall for the same period (1979–2017).

### 2.2 | Methods

To identify the synoptic circulation patterns over Southern Africa associated with rainfall over the SWC in South Africa, we applied self-organizing maps (SOMs) analysis to ERA-INT daily 850 hPa geopotential height datasets using all days from March to October for the period 1979–2017 over a small Southern African domain extending from  $0^\circ$  to  $34.5^\circ\text{E}$  and  $19.5$  to  $45^\circ\text{S}$ . This domain is large enough to capture the major synoptic features such as the subtropical anticyclones and the westerly winds that influence rainfall variability over the SWC. It is similar to the domain used by Wolski *et al.* (2018) to assess rainfall variability over Cape Town based on SOMs. 850 hPa geopotential height is considered the best single predictor field characterizing rainfall variability over Southern Africa (Landman and Goddard, 2002).

SOM is an artificial neural network-based cluster analysis that identifies frequently occurring spatial patterns in multidimensional datasets by clustering and reducing their initial dimensions (Kohonen, 1990, 2013; Vesanto and Alhoniemi, 2000; Johnson, 2013). A SOM analysis organizes its input vectors into characteristic nodes or patterns by grouping similar patterns closer together

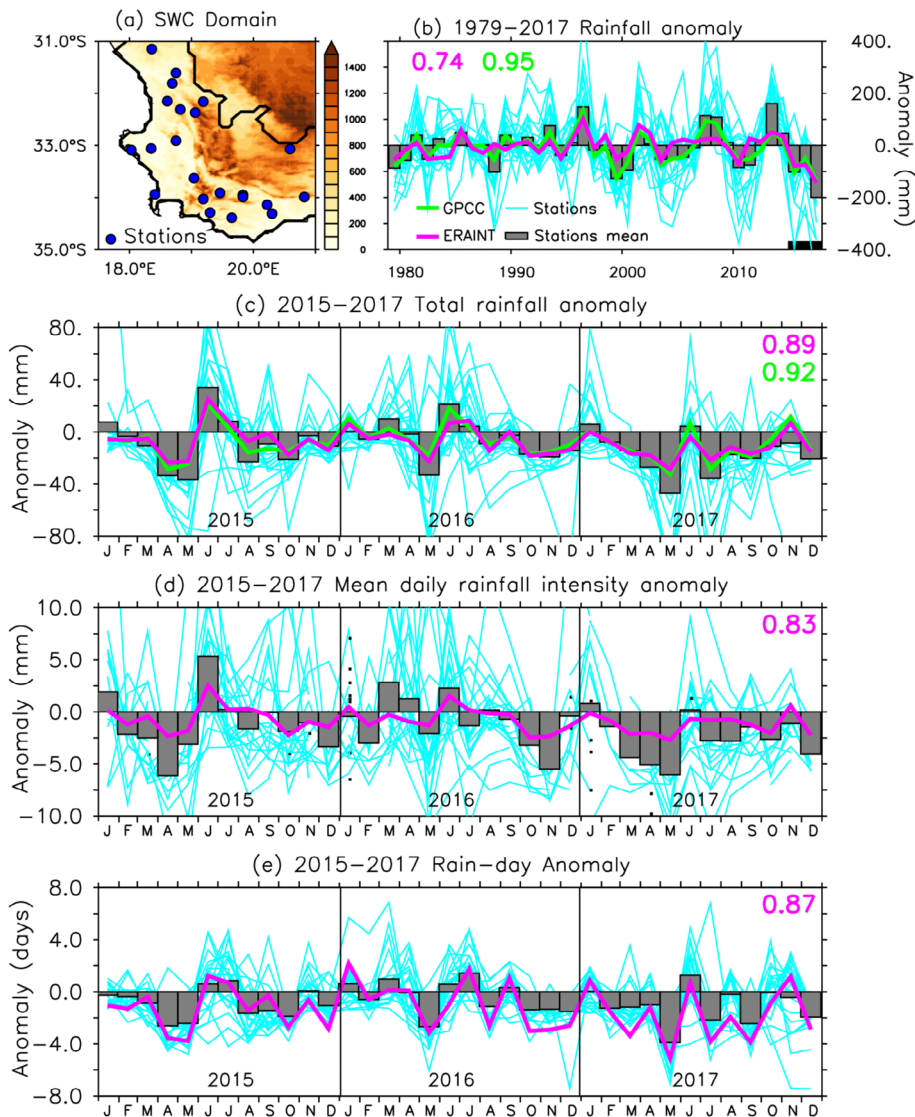


**FIGURE 1** (a) The South West of the Western Cape (SWC) domain in South Africa showing the topography (meter) and the location of the 22 rainfall stations used in this study; (b) total annual rainfall anomaly (mm) for 1979–2017 for the 22 stations, GPCC, and ERAINT datasets. Anomalies of (c) monthly rainfall (mm), (d) mean daily rainfall intensity (mm), and (e) rain day for the 22 stations and ERAINT data for each year in the drought period. The thin lines represent the individual stations, the bars the mean anomalies for all stations, and the thick lines represent GPCC and ERAINT. All anomalies are calculated inland over the SWC domain in (a) with reference to 1981–2010 long-term climatology. The area shaded in black in (b) on the horizontal axis represents the drought period (2015–2017). The numbers in the upper left-hand corner (a) and upper right-hand corner (b–e) represent the correlation between stations mean and each of GPCC and ERAINT datasets [Colour figure can be viewed at [wileyonlinelibrary.com](http://wileyonlinelibrary.com)]

and non-similar patterns apart away, typically within a 2-dimensional array of states (Sheridan and Lee, 2011). SOMs have been extensively used in atmospheric studies as a synoptic classification approach to characterize atmospheric circulation states and how they relate to the local climate (Hewitson and Crane, 2002; MacKellar *et al.*, 2009; Lennard and Hegerl, 2015; Henderson *et al.*, 2016).

We used SOM software from the Laboratory of Computer and Information Science at Helsinki University of Technology (Kohonen *et al.*, 1996). Due to the relatively small size of our data and to reduce the level of circulation archetypes generalization, we initialised the data in the SOM algorithm with  $5 \times 6$  nodes (30 nodes) with a rectangular topology and one phase of 50,000 iterations.

We analysed the anomalies during the drought period (2015–2017) compared to the historical long-term climatological reference (1981–2010), assessing the frequency of the atmospheric circulation states identified by the SOM algorithm. That frequency was expressed by the number of

node-days, that is, days when a given node occurred, in a month. To provide understanding of conditions underlying the drought, but not necessarily captured by the frequency of synoptic states, we examined anomalies of rainfall characteristics associated with each of the states identified by the SOM. We calculated anomalies in rain-day frequency, mean rainfall intensity, and total rainfall for each node on a monthly basis, with the first and the second calculated per node-days. We also determined the composite of moisture flux and CAPE over Southern Africa with a focus on the SWC domain on the node-days.

### 3 | RESULTS

#### 3.1 | Rainfall anomalies in 2015–2017

The 2015–2017 SWC drought had a multi-year character, which contributed strongly to its impact on Cape Town

water resources and the resulting water crisis. Total annual rainfall in each of the 2015–2017 years was lower than the long-term average, with the strongest anomaly in 2017 (Figure 1b), both in our station data, GPCC, and ERAINT. This analysis agrees with previous studies on the drought (Sousa *et al.*, 2018; Abba Omar and Abiodun, 2020) and provides a context for more specific analyses. On a monthly basis, the anomaly manifested differently between seasons, but the pattern of seasonal anomalies was similar between years (Figure 1c). While rainfall in the core of the winter rainfall season (June–July: “JJ”) was near or above normal, in the shoulder season months (March–May: “MAM” and August–October: “ASO”), rainfall was below normal in 2015 and 2017, and near normal in 2016. The total rainfall anomaly in the shoulder seasons was caused by a combination of the lower frequency of rain-days and lower intensity of daily rainfall events (Figure 1d,e).

### 3.2 | SOM circulation patterns

The weather in South-Western Cape is influenced by the interaction of three factors reflecting subtropical and temperate influences on the region's climate (Reason, 2017): (a) strength of subsidence associated with South Atlantic and South Indian subtropical anticyclones, with the related zonal positioning of the mid-latitude westerlies, (2) thermal heating over the land leading to sub-continental low pressure system, and (3) the passage of the westerly wave. A more northerly position of both the westerlies and high pressure over the continent are characteristic of winter (June–August or JJA), while a southerly position of the westerlies and low pressure over the continent are characteristic of summer (DJF); the westerly wave disturbance manifests time scale of 6–8 days.

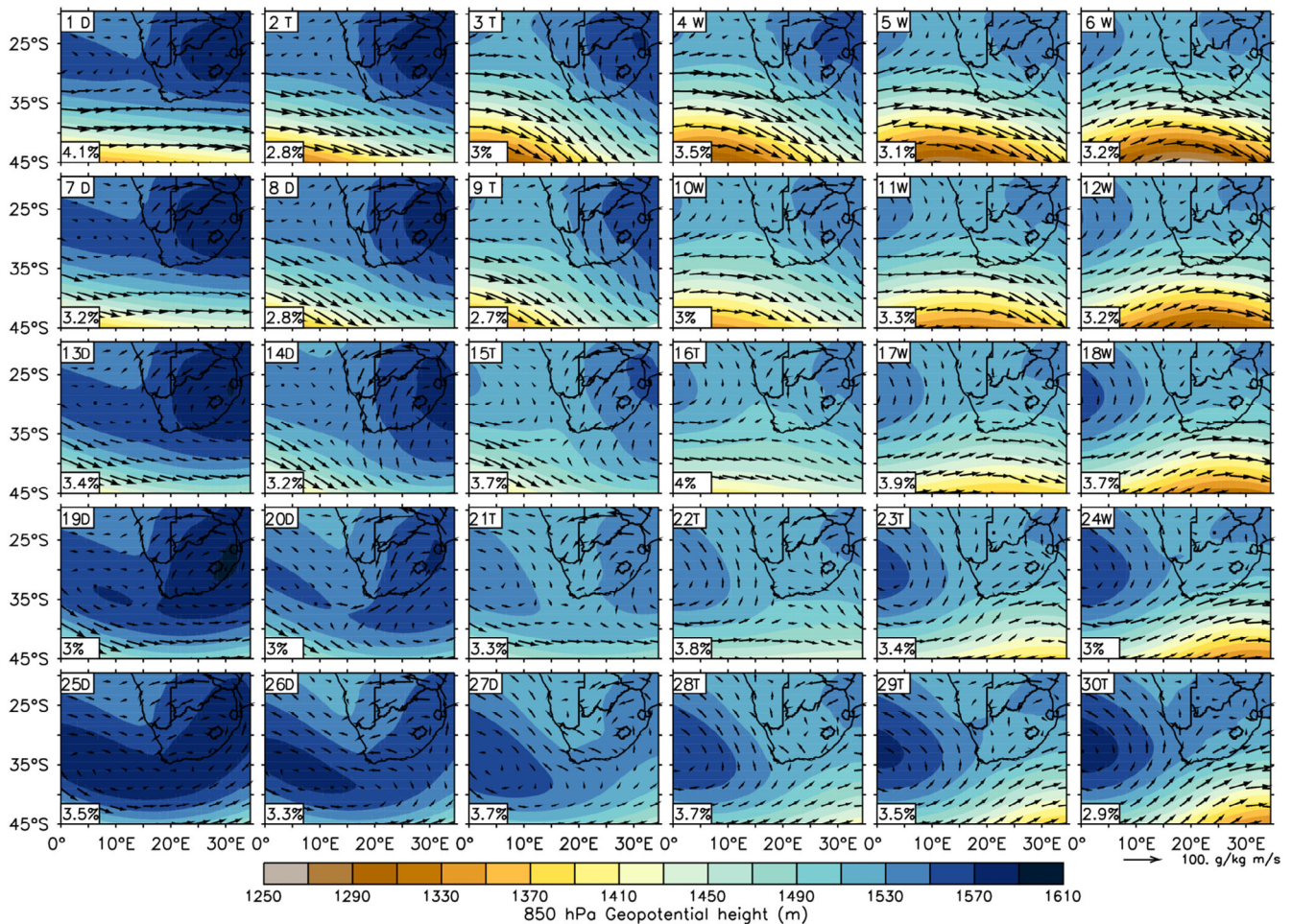


**FIGURE 2** Daily (March–October) 850 hPa geopotential heights for 1979–2017 classified using the self-organizing maps (SOM) with 30 nodes. The arrows represent the moisture flux ( $\text{g}\cdot\text{kg}^{-1}\cdot\text{m}\cdot\text{s}^{-1}$ ) at 850 hPa associated with each node. In the lower left-hand corner of each panel is the frequency of occurrence of each SOMs node over the study period; while the number in the upper left-hand corner of each node indicates the node number and position in the SOMs array. The letter in the upper left-hand corner of each node indicates the circulation types represented by that node: ‘D’ for dry circulation nodes, ‘T’ for transition circulation nodes, and ‘W’ for the rain-bearing circulation nodes [Colour figure can be viewed at [wileyonlinelibrary.com](http://wileyonlinelibrary.com)]

Rainfall producing nodes (winter-time conditions) are represented in the SOM analysis by nodes in the top right corner of the SOM array (Figure 2). The westerly wave manifests strongly in winter circulation, with a cyclical transition in the vicinity of the African continent between the low pressure system associated with the mid-latitude cyclones (node 6), followed by southerly meridional flow (node 30), a ridging high pressure system connecting Atlantic and Indian Ocean lows (node 25) and circulation dominated by subtropical highs at the wave's trough (node 1).

The SOM in Figure 2 does not capture typical summer conditions as November, December, January, and February were not included in data used to develop it, but it does represent transitional (spring/autumn) conditions, with the westerlies in their more southerly position, and with weak, or no continental low. Those conditions are represented by nodes occupying the central part of the SOM, with the northward position of the westerlies increasing from bottom to top of the array. The

westerly wave still manifests within those nodes (e.g., nodes 21–23, Figure 2).

Several specific circulation conditions are occurring within this basic pattern, such as cut-off lows and west coast troughs (Tyson and Preston-Whyte, 2000), but these are less frequent and manifest by anomalies at smaller scales, and are thus not captured within the relatively large scale and generalized SOM patterns in Figure 2. Those circulation types occur most frequently in the transition (spring/autumn) seasons (Tyson and Preston-Whyte, 2000), and fall under the nodes in the central part of the SOM.

In the core winter season (JJA), rain-bearing conditions are associated with northerly positions of the westerlies and convergence occurring at the front of the cyclonic disturbance (exemplified by node 6 in Figures 2 and 3), while dry conditions are associated with the strong pressure ridge (nodes 7, 8, 13, 14, 19, 20, and 25–27) and near-parallel zonal flow (indicating a lack of cyclonic disturbance) in the westerlies (e.g., node 1). In

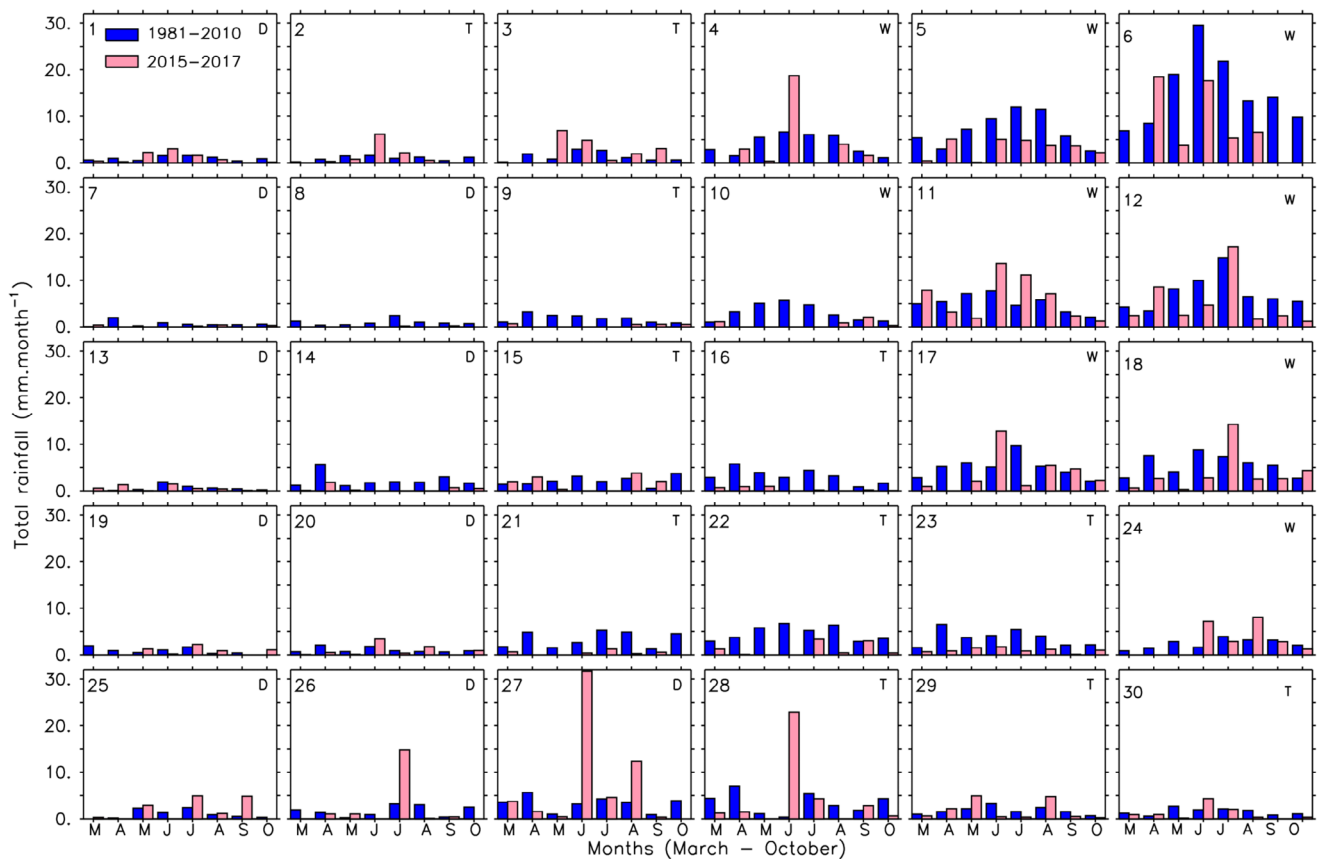


**FIGURE 3** Observed total monthly rainfall ( $\text{mm}\cdot\text{month}^{-1}$ ) that occurred on days characterized by the circulation states represented in Figure 2, during the climatological reference period (1981–2010; blue bars) and the drought period (2015–2017; orange bars). The number in the upper left-hand corner of each node indicates the node number and position in the SOMs array. The letter in the upper right-hand corner of each node indicates the circulation types represented by that node: 'D' for dry circulation nodes, 'T' for transition circulation nodes, and 'W' for the rain-bearing circulation nodes [Colour figure can be viewed at [wileyonlinelibrary.com](http://wileyonlinelibrary.com)]

the transition seasons, our SOM does not clearly distinguish rain-bearing from dry circulation types, likely due to its inability to resolve the particular patterns associated with rain, that is, west coast troughs and cut-off lows. These can likely fall under several regional circulation types within the central part of the SOM. Only the better-defined circulation of prefrontal conditions (nodes 8–9 and nodes 14–15) are characterized by dry conditions.

### 3.3 | Frequency of SOM circulation patterns under climatological and drought conditions

The similarity in the frequency of occurrence of the synoptic states across the SOM nodes during the March–October season of 1979–2017 (Figure 2)—as shown by the number in the lower left-hand corner—is an artefact of SOM algorithm, which tends to equalize frequencies of nodes describing the calibration data. The distribution of the frequency of the synoptic circulation types across the

SOM array during the climatological reference period (1981–2010) varies between months, however, reflecting different synoptic conditions predominant during different phases of the seasonal cycle (Figure 4), with three regimes, described below.

In March, April, and October, the highest frequency of occurrence of the synoptic types is located in the centre of the SOM array, reflecting the domination of transitional circulation types over the SWC (Figure 4). In JJA, under a winter regime, nodes along the right, top and left boundary of the SOM array occur the most frequently. May and September represent a mixed regime, where both winter and transitional seasons conditions occur.

The anomalies in the frequency of the circulation types in 2015–2017 relative to the climatological reference (1981–2010) varied between months (Figure 4). In March and April (transitional regime), there was a higher frequency of states occurring typically in winter, including the low-pressure systems associated with cold front and thus rainfall over SWC (node 6). May, however, had distinctly fewer occurrences of that state, with markedly

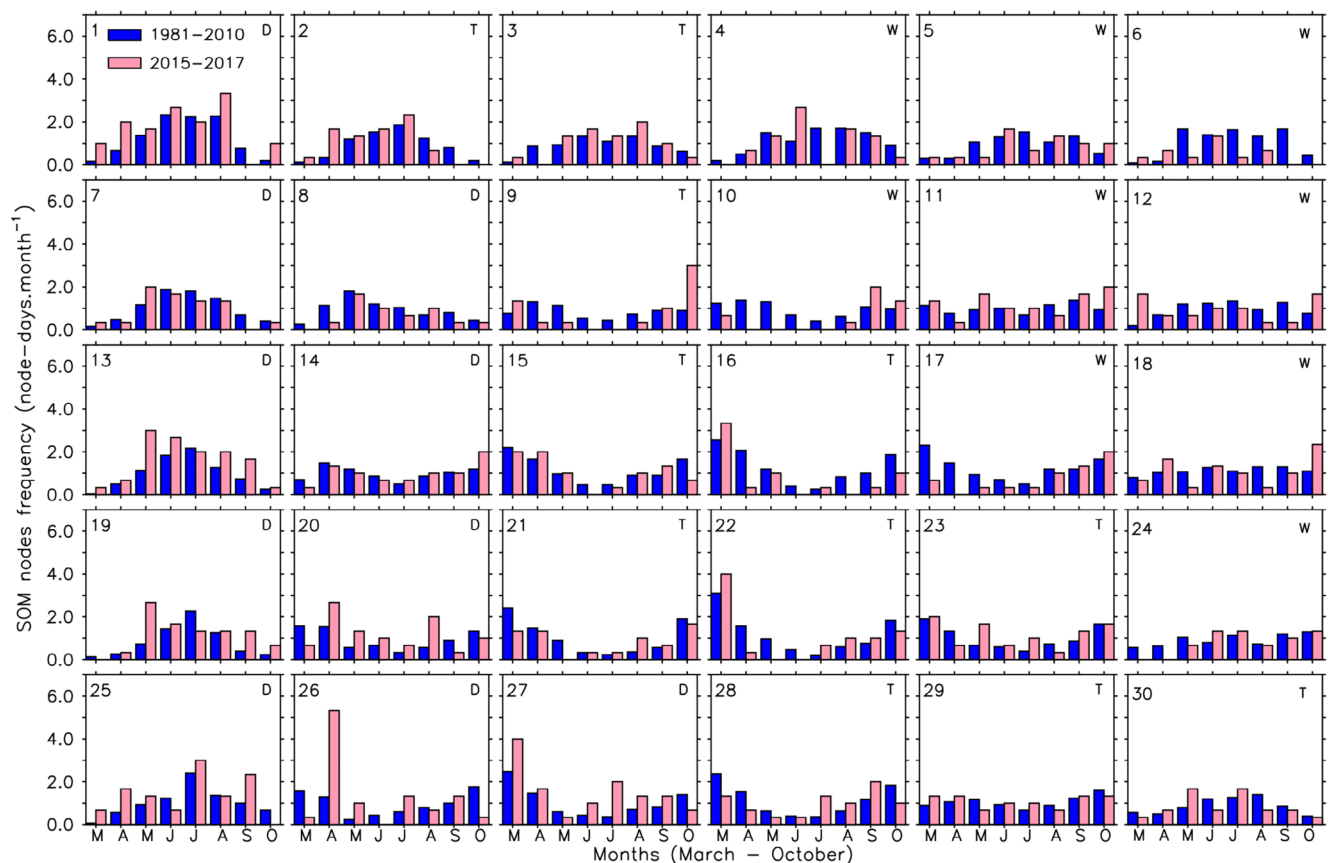


**FIGURE 4** Frequency of occurrence of SOM nodes shown in Figure 2 during the climatological reference period (1981–2010; blue or bark bars) and the drought period (2015–2017; pink or light bars). The number in the upper left-hand corner of each node indicates the node number and position in the SOMs array. The letter in the upper right-hand corner of each node indicates the circulation types represented by that node: ‘D’ for dry circulation nodes, ‘T’ for transition circulation nodes, and ‘W’ for the rain-bearing circulation nodes [Colour figure can be viewed at [wileyonlinelibrary.com](http://wileyonlinelibrary.com)]

higher frequency of states characterized by high pressure south of the continent (nodes 19–20 and 25–26). June had a lower frequency of the transitional regime states, but no marked anomaly in the frequency of the typical winter regime circulation states. July and August had a higher frequency of transitional regime states characterized by the more southerly position of the mid-latitude low pressure and the westerlies (nodes in the bottom-central part of the SOM). Overall, the shoulder season months were characterized by an increase in dry and transitional circulation types, while the core winter months were dominated by wet and transition circulation types, resulting in lower rainfall anomalies (Figures 3 and 4).

### 3.4 | Rainfall characteristics associated with SOM circulation patterns

The total monthly rainfall contributed by individual circulation states, during the climatological reference period

(1981–2010), is high for the nodes associated with the strong winter-type frontal disturbance in the westerlies (top right-hand corner of the SOM array, Figure 3). Rainfall is lower for the transitional circulation types (nodes to the right of the diagonal) and very low or zero for the dry circulation types (top left-hand corner).

During the 2015–2017 drought, there was a general decrease in rainfall contributed by rain-bearing states (with both high and moderate rainfall) except in April, when rainfall contributed by nodes 4–6 and 12 increased (Figure 3). In May, the contribution of the “wettest” states was particularly low.

In order to disentangle the effects on rainfall anomaly of change in frequency of synoptic states as captured by SOM from other (thermodynamic) effects, we illustrate climatological and drought-period characteristics of rainfall on “node days”. Figure S1 shows rainfall intensity expressed as the mean rainfall calculated for rain days (rainfall  $\geq 1 \text{ mm-day}^{-1}$ ) per node day, and Figure 5 shows the frequency of rain days calculated as a proportion of node days.

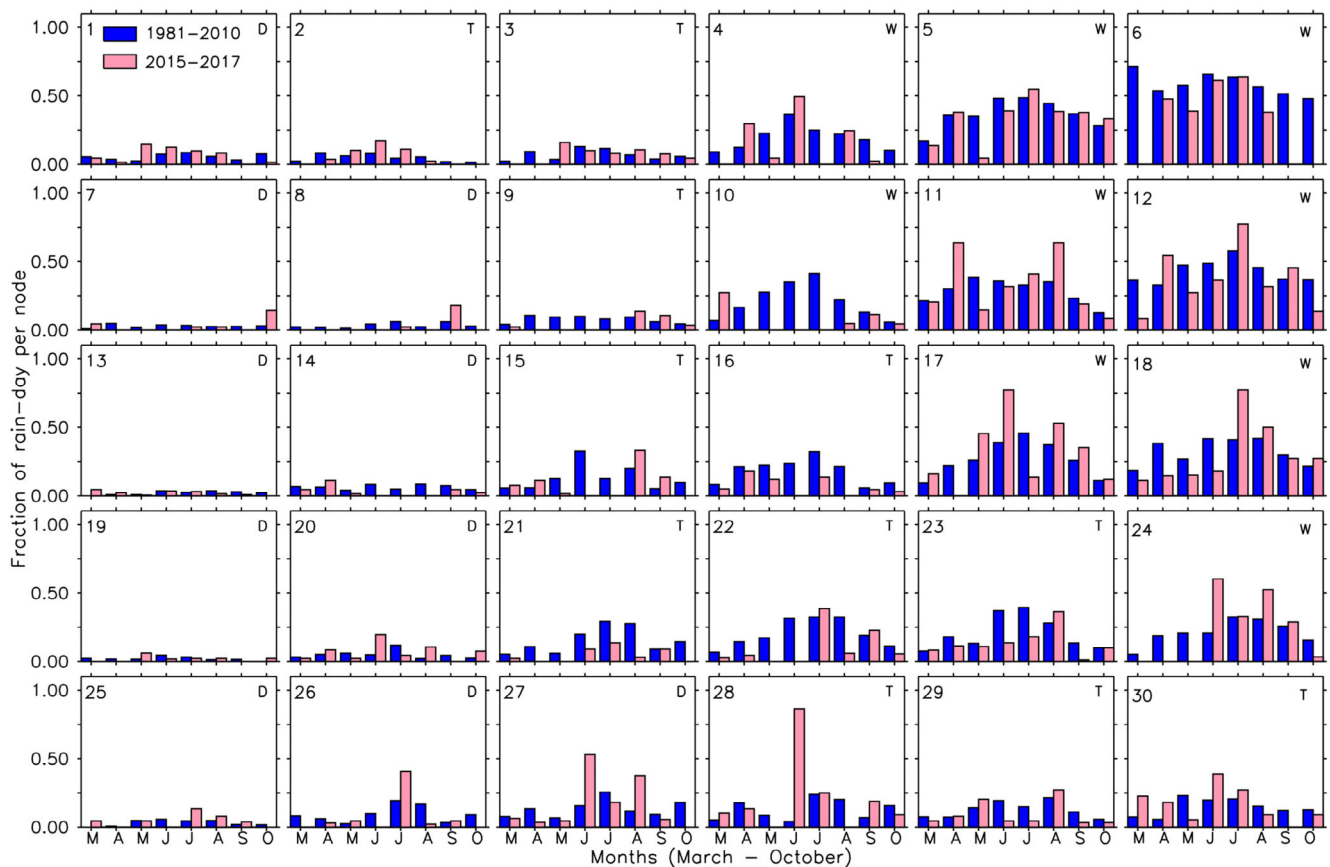


**FIGURE 5** Fraction of rain days per node-days, that is, days characterised by the circulation states represented in Figure 2 during the climatological reference period (1981–2010; blue or dark bars) and the drought period (2015–2017; pink or light bars). The number in the upper left-hand corner of each node indicates the node number and position in the SOMs array. The letter in the upper right-hand corner of each node indicates the circulation types represented by that node: ‘D’ for dry circulation nodes, ‘T’ for transition circulation nodes, and ‘W’ for the rain-bearing circulation nodes [Colour figure can be viewed at [wileyonlinelibrary.com](http://wileyonlinelibrary.com)]

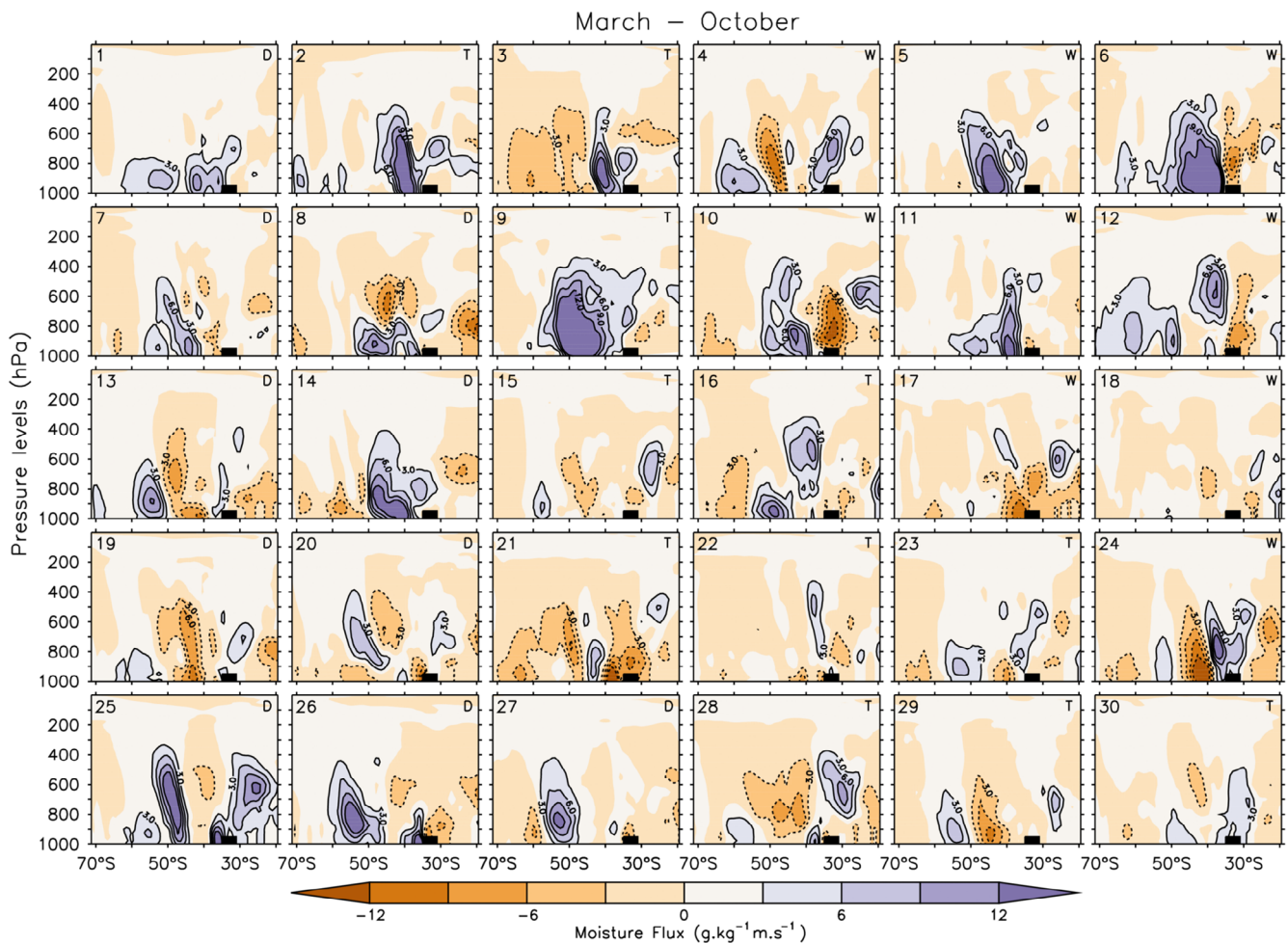


**FIGURE 6** Latitude-height cross-section of moisture flux ( $\text{g}\cdot\text{kg}^{-1}\cdot\text{m}\cdot\text{s}^{-1}$ ) averaged between  $17.5\text{--}21^\circ\text{E}$  showing the 2015–2017 moisture flux anomalies in March–October for days characterised by the circulation states represented in Figure 2. The black box on the horizontal axis represents the SWC region. The number in the upper left-hand corner of each node indicates the node number and position in the SOMs array. The letter in the upper right-hand corner of each node indicates the circulation types represented by that node: ‘D’ for dry circulation nodes, ‘T’ for transition circulation nodes, and ‘W’ for the rain-bearing circulation nodes. The contour interval is  $3\text{ g}\cdot\text{kg}^{-1}\text{ m}\cdot\text{s}^{-1}$  [Colour figure can be viewed at [wileyonlinelibrary.com](http://wileyonlinelibrary.com)]

The climatological (1981–2010) rainfall intensity and frequency patterns are similar to those of total rainfall (cf. Figures S1 and 5 with Figure 3), i.e., the highest intensity and frequency is associated with node 6, moderate values with the top-right, and lowest or null values with the top-left and left-hand side section of the SOM array. There seem to be higher rainfall intensities associated with the same circulation patterns occurring in July than in other months. Also, there are some differences in rain days per node day between months—for a number of “drier” circulation patterns (nodes 20, 26, 27), there are fewer rain days in the transitional seasons than when those conditions occur in core winter (JJA). Those differences likely express seasonal and systematic differences in rainfall drivers that are not captured by the SOM of 850 hPa geopotential field.

During the 2015–2017 drought in the SWC, the shape of the distribution of rain days per node day remained similar to its climatology (Figures 5) but with fewer rain days per node day. Also, in all months, the decrease in the proportion of rain days per node day was widespread across the SOM array with; however, some increases in nodes with rain-bearing circulation states in April and July. The per node day rain also decreased during the 2015–2017 drought, like rain days per node day (Figure S1). However, node 27, a climatologically dry node, was wetter than normal during the drought (Figure S1), which may probably be associated with cut-off lows (Abba Omar and Abiodun, 2020).

It appears that the lower rainfall in the drought years was from both a reduction in the number of rain-bearing synoptic states and the reduction in the amount of rain falling when these states did occur.

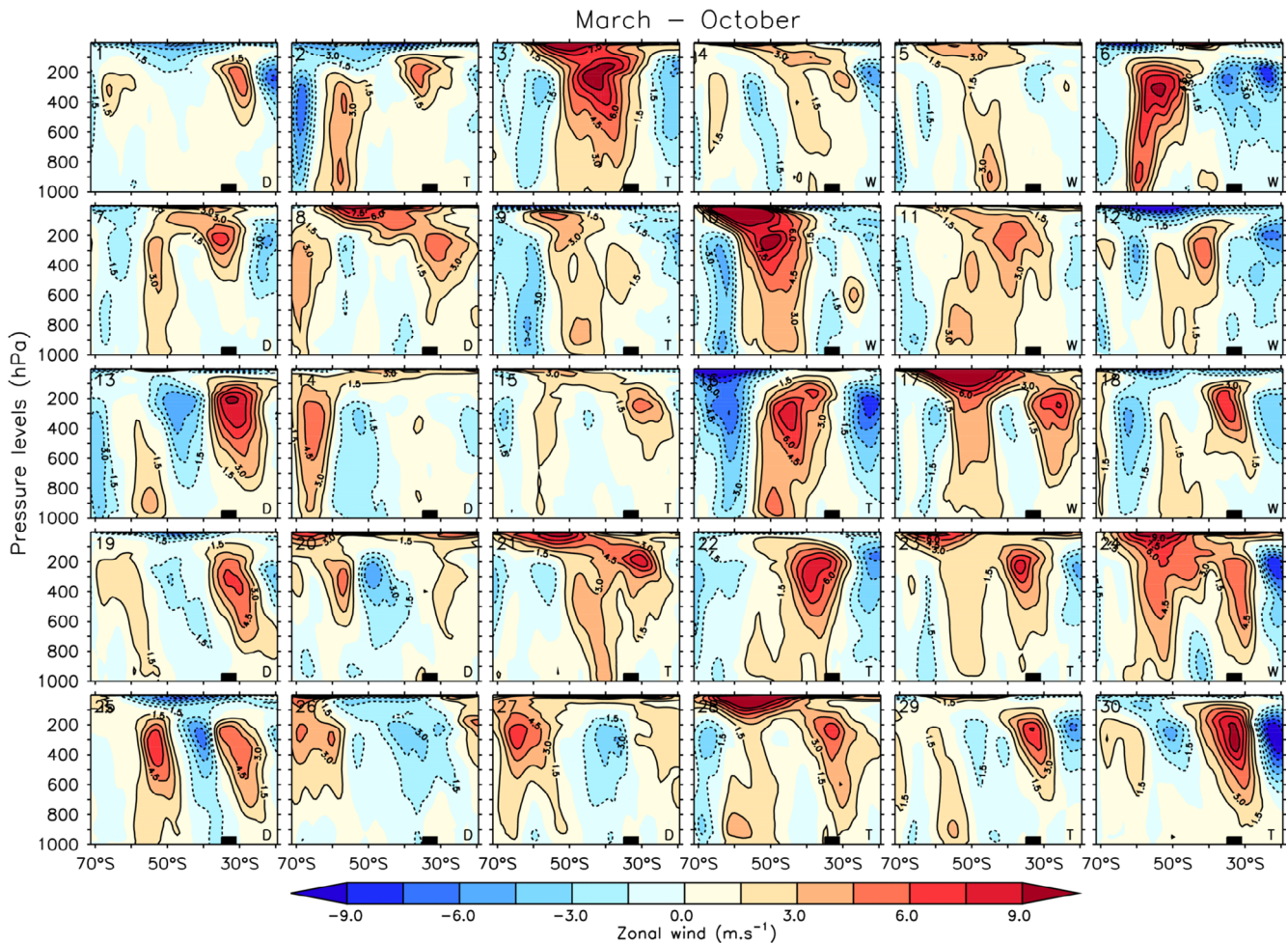


**FIGURE 7** Latitude-height cross-section of zonal wind ( $\text{m}\cdot\text{s}^{-1}$ ) averaged between  $17.5\text{--}21^\circ\text{E}$  showing the 2015–2017 zonal wind anomalies in March–October for days characterised by the circulation states represented in Figure 2. The black box on the horizontal axis represents the SWC region. The number in the upper left-hand corner of each node indicates the node number and position in the SOMs array. The letter in the lower right-hand corner of each node indicates the circulation types represented by that node: ‘D’ for dry circulation nodes, ‘T’ for transition circulation nodes, and ‘W’ for the rain-bearing circulation nodes. The contour interval is  $1.5\text{ m}\cdot\text{s}^{-1}$  [Colour figure can be viewed at [wileyonlinelibrary.com](http://wileyonlinelibrary.com)]

### 3.5 | Variables expressing local state of the atmosphere

Figure 6 shows the latitude-height cross section of anomalies in moisture flux across the SOM array during the 2015–2017 drought. Overall, rain-bearing circulation types are characterized by positive moisture flux anomalies further south and negative anomalies over the SWC. In most wet nodes (5, 6, and 10–12) the positive moisture flux anomaly is located south of the SWC over the ocean while, in nodes 17 and 18, there were no latitudinal shifts, simply a reduction in overall flux (Figure 6). Analysis on the seasonal level (March–May, June–July, and August–October) shows similar results especially in the shoulder seasons (Figures S2–S4). The positive anomaly in moisture flux to the south is concordant with

anomalies of westerly winds which during 2015–2017 were anomalously strong south of the SWC (over ocean) and weaker over the SWC, especially in rain bearing nodes (Figures 7, S5–S7).

During the 2015–2017 drought, there was a general decrease in CAPE over the SWC across the SOM nodes (Figures 8 and S8). CAPE anomalies depicted some similarities with rainfall anomalies over the SWC. For example, like total rainfall, CAPE increased in rain-bearing circulation types in April (nodes 4–6), while it decreased in May (Figures 4 and 8). Also, in March–June, August, and October rainfall decreased (Figures 4 and S1) in most nodes with transitional circulation types together with CAPE (Figure 8). The decreases in CAPE, during the drought period, would influence convection over the SWC, which in return could influence droughts, on a

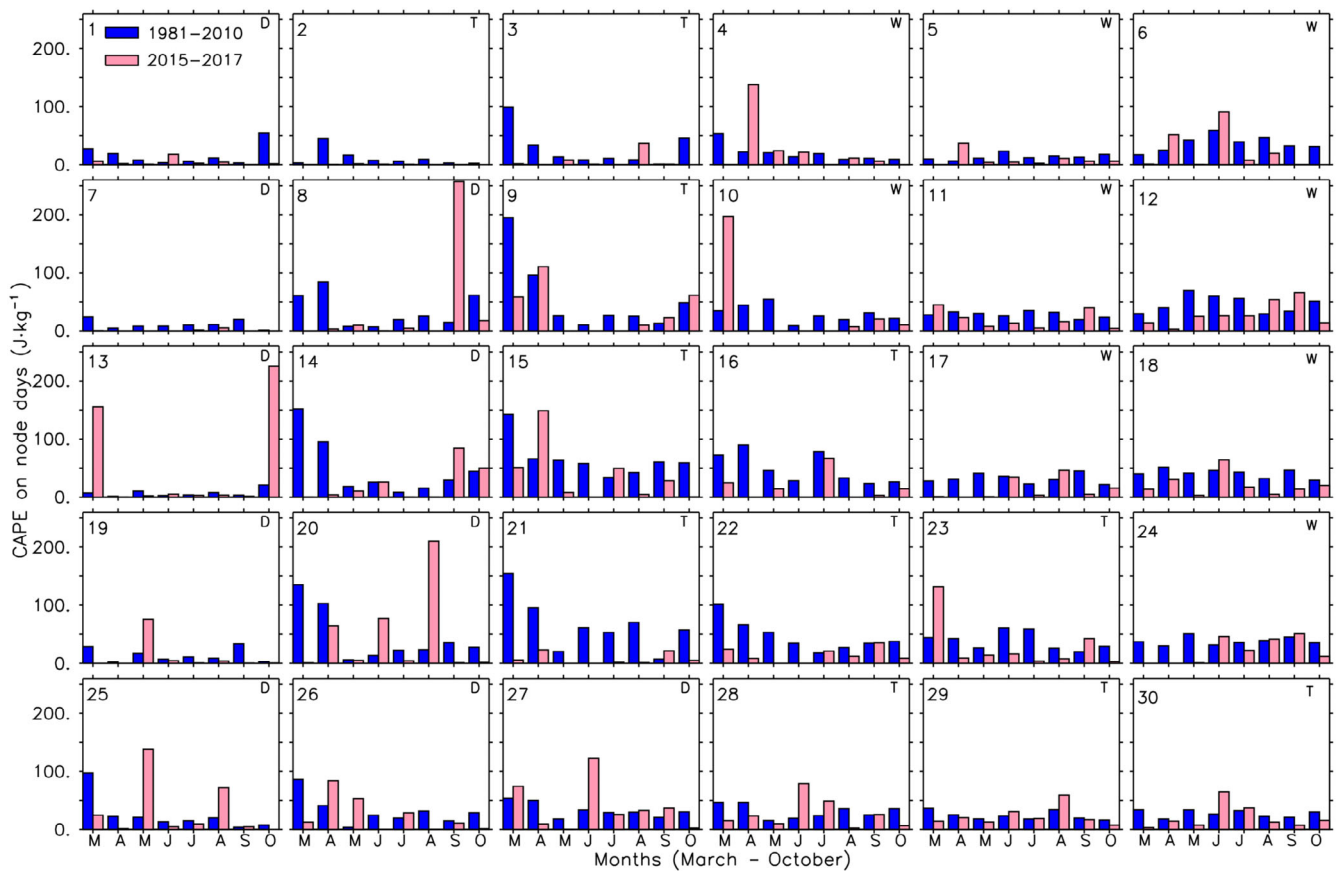


**FIGURE 8** Convective available potential energy (CAPE,  $\text{J}\cdot\text{kg}^{-1}$ ) over the SWC on days characterised by the circulation states represented in Figure 2 during the climatological reference period (1981–2010; blue or dark bars) and the drought period (2015–2017; pink or light bars). The number in the upper left-hand corner of each node indicates the node number and position in the SOMs array. The letter in the upper right-hand corner of each node indicates the circulation types represented by that node: ‘D’ for dry circulation nodes, ‘T’ for transition circulation nodes, and ‘W’ for the rain-bearing circulation nodes. [Colour figure can be viewed at [wileyonlinelibrary.com](http://wileyonlinelibrary.com)]

long-time scale, and extreme weather events, on a shorter time scale (Riemann-Campe *et al.*, 2011).

## 4 | DISCUSSION AND CONCLUSIONS

This study analysed the frequency of circulation types, rainfall characteristics, along with associated local moisture flux and CAPE, during the 2015–2017 drought over the SWC compared to the previous (1981–2010) years. We identified in this study two factors associated with reduced rainfall during the drought. The first is the decrease in the occurrence frequency of synoptic circulation states associated with rain-bearing frontal systems over the SWC and the increased frequency of dry and transitional circulation types. Second is the decrease in the amount of rainfall delivered when rain-bearing synoptic types were present. When rain-bearing nodes did occur, they tended to be accompanied by a southward

shift of westerlies and moisture limiting the influx of moisture into the region. During the 2015–2017 drought, winter months were particularly characterized by persistent high-pressure fields with frequent ridging of the two SAH and SIH over the sub-continent suppressing rainfall (intensity, frequency, and duration) over the SWC. This agrees with Burls *et al.* (2019), who reported a link between rain-bearing fronts and rainfall duration over the SWC. The southward shift of westerlies and the persistence of high pressure over the region also influenced atmospheric moisture, which decreased during the drought years, especially in the shoulder seasons over the region. Additionally, the decrease of CAPE, during the drought may have helped reduce the convective potential over the SWC, further suppressing rainfall.

Our results suggest that a decrease in the frequency of synoptic states associated with rain-bearing circulation types was a major contributor to the 2015–2017 drought in the SWC of South Africa, as it affected daily rainfall characteristics (per-node rainfall amount, total monthly

rainfall, and rain-day frequency). This suggests that the significant upward (downward) trend of dry (wet) circulation types in most seasons (including winter) during 1979–2009 over Cape Town, reported by Lennard and Hegerl (2015) at one Cape Town station, might have continued until 2017, affecting the rainfall frequency associated with these circulation types. Our results also align with those of, Burls *et al.* (2019) who identified longer-term drought trends linked to the combined influence of a long-term (1910–2017) decrease of rainfall day frequency associated with a more recent (1979–2017) deficit in rainfall intensity. All these in conjunction with less moisture influx into SWC, less westerlies reaching SWC, and decreases in CAPE during 2015–2017 drove the rainfall deficit, which led to the SWC drought in 2015–2017.

In conclusion, it is important to highlight that the drought was the result of the combination of several factors, the most important being the combined decrease in rain-bearing circulation types and the increase in dry circulation types, which influenced the decline in the local rainfall (frequency and intensity). Also, the rainfall associated with rain-bearing circulation types decreased during the 2015–2017 drought due to a southward shift in westerlies and less moisture influx into the SWC region. Further studies may, therefore, improve these findings by analysing the multi-year drought (2015–2017) as a compound weather event to determine its dominant drivers.

## ACKNOWLEDGEMENTS

The authors acknowledge the support received from the BNP Paribas Climate Foundation and the AXA Research Fund, who both support the AXA Research Chair Programme in African Climate Risk at the University of Cape Town. We would also like to acknowledge the Southern African Systems Analysis Centre (SASAC) and funding provided by the South African National Research Foundation (NRF) and Department of Science and Technology (DST). Computational resources were provided by the Centre for High Performance Computing (CHPC, South Africa).

## CONFLICT OF INTEREST

The authors declare no conflict of interest.

## ORCID

Romarc C. Odoulami  <https://orcid.org/0000-0001-8228-1608>

Piotr Wolski  <https://orcid.org/0000-0002-6120-6593>

Mark New  <https://orcid.org/0000-0001-6082-8879>

## REFERENCES

Abba Omar, S. and Abiodun, B.J. (2020) Characteristics of cut-off lows during the 2015–2017 drought in the Western Cape,

South Africa. *Atmospheric Research*, 235, 104772. <https://doi.org/10.1016/j.atmosres.2019.104772>.

Blamey, R. and Reason, C.J.C. (2007) Relationships between Antarctic sea-ice and South rainfall, African winter. *Climate Research*, 33, 183–193.

Botai, C., Botai, J., de Wit, J., Ncongwane, K. and Adeola, A. (2017) Drought characteristics over the Western Cape Province, South Africa. *Water*, 9(11), 876. <https://doi.org/10.3390/w9110876>.

Burls, N.J., Blamey, R.C., Cash, B.A., Swenson, E.T., al, F.A., Bopape, M.-J.M., Straus, D.M. and Reason, C.J.C. (2019) The Cape Town “day zero” drought and Hadley cell expansion. *NPJ Climate and Atmospheric Science*, 2(1), 27. <https://doi.org/10.1038/s41612-019-0084-6>.

Cook, B.I., Smerdon, J.E., Seager, R. and Coats, S. (2014) Global warming and 21st century drying. *Climate Dynamics*, 43(9–10), 2607–2627. <https://doi.org/10.1007/s00382-014-2075-y>.

DEA (Department of Environmental Affairs). (2013). Long-Term Adaptation Scenarios Flagship Research Programme (LTAS) for South Africa. Climate Trends and Scenarios for South Africa. Pretoria, South Africa.

Dee, D.P., Uppala, S.M., Simmons, A.J., Berrisford, P., Poli, P., Kobayashi, S., Andrae, U., Balmaseda, M.A., Balsamo, G., Bauer, P., Bechtold, P., Beljaars, A.C.M., van de Berg, L., Bidlot, J., Bormann, N., Delsol, C., Dragani, R., Fuentes, M., Geer, A.J., Haimberger, L., Healy, S.B., Hersbach, H., Hólm, E. V., Isaksen, I., Kållberg, P., Köhler, M., Matricardi, M., McNally, A.P., Monge-Sanz, B.M., Morcrette, J.-J., Park, B.-K., Peubey, C., de Rosnay, P., Tavolato, C., Thépaut, J.-N. and Vitart, F. (2011) The ERA-Interim reanalysis: configuration and performance of the data assimilation system. *Quarterly Journal of the Royal Meteorological Society*, 137(656), 553–597. <https://doi.org/10.1002/qj.828>.

Feng, S. and Fu, Q. (2013) Expansion of global drylands under a warming climate. *Atmospheric Chemistry and Physics*, 13(19), 10081–10094. <https://doi.org/10.5194/acp-13-10081-2013>.

Henderson, G.R., Barrett, B.S. and South, K. (2016) Eurasian October snow water equivalent: using self-organizing maps to characterize variability and identify relationships to the MJO. *International Journal of Climatology*, 37(2), 596–606. <https://doi.org/10.1002/joc.4725>.

Hewitson, B.C. and Crane, R.G. (2002) Self-organizing maps: applications to synoptic climatology. *Climate Research*, 22, 13–26.

Johnson, N.C. (2013) How many ENSO flavors can we distinguish? *Journal of Climate*, 26(13), 4816–4827. <https://doi.org/10.1175/JCLI-D-12-00649.1>.

Kohonen, T. (1990) The self-organizing map. *Proceedings of the IEEE*, 78(9), 1464–1480. <https://doi.org/10.1109/5.58325>.

Kohonen, T. (2013) Essentials of the self-organizing map. *Neural Networks*, 37, 52–65. <https://doi.org/10.1016/j.neunet.2012.09.018>.

Kohonen, T., Hynninen, J., Kangas, J., Laaksonen, J. (1996). SOM\_PAK: The Self-Organizing Map Program Package. *Report A31*. Espoo, Finland.

Landman, W.A. and Goddard, L. (2002) Statistical recalibration of GCM forecasts over southern Africa using model output statistics. *Journal of Climate*, 15(15), 2038–2055. [https://doi.org/10.1175/1520-0442\(2002\)015<2038:SROGFO>2.0.CO;2](https://doi.org/10.1175/1520-0442(2002)015<2038:SROGFO>2.0.CO;2).

- Lehner, F., Coats, S., Stocker, T.F., Pendergrass, A.G., Sanderson, B. M., Raible, C.C. and Smerdon, J.E. (2017) Projected drought risk in 1.5°C and 2°C warmer climates. *Geophysical Research Letters*, 44(14), 7419–7428. <https://doi.org/10.1002/2017GL074117>.
- Lennard, C. and Hegerl, G. (2015) Relating changes in synoptic circulation to the surface rainfall response using self-organising maps. *Climate Dynamics*, 44(3–4), 861–879. <https://doi.org/10.1007/s00382-014-2169-6>.
- MacKellar, N., Tadross, M. and Hewitson, B. (2009) Synoptic-based evaluation of climatic response to vegetation change over southern Africa. *International Journal of Climatology*, 30(5), 774–789. <https://doi.org/10.1002/joc.1925>.
- Mahlalela P. T., Blamey R. C., Reason C. J. C. (2019) Mechanisms behind early winter rainfall variability in the southwestern Cape, South Africa. *Climate Dynamics*, 53 (1-2), 21–39. <http://dx.doi.org/10.1007/s00382-018-4571-y>.
- Moise, A.F. and Hudson, D.A. (2008) Probabilistic predictions of climate change for Australia and southern Africa using the reliability ensemble average of IPCC CMIP3 model simulations. *Journal of Geophysical Research*, 113(D15113), 1–26. <https://doi.org/10.1029/2007JD009250>.
- Niang, I., Ruppel, O.C., Abdrabo, M.A., Essel, A., Lennard, C., Padgham, J. and Urquhart, P. (2014) Africa. In: Barros, V.R., Field, C.B., Dokken, D.J., Mastrandrea, M.D., Mach, K.J., Bilir, T.E., Chatterjee, M., Ebi, K.L., Estrada, Y.O., Genova, R. C., Girma, B., Kissel, E.S., Levy, A.N., MacCracken, S., Mastrandrea, P.R. and White, L.L. (Eds.) *Climate Change 2014: Impacts, Adaptation, and Vulnerability. Part B: Regional Aspects. Contribution of Working Group II to the Fifth Assessment Report of the Intergovernmental Panel on Climate Change*. Cambridge, United Kingdom/New York, NY: Cambridge University Press, pp. 1119–1265.
- Otto, F.E.L., Wolski, P., Lehner, F., Tebaldi, C., van Oldenborgh, G. J., Hogesteeger, S., Singh, R., Holden, P., Fučkar, N.S., Odoulami, R.C. and New, M. (2018) Anthropogenic influence on the drivers of the Western Cape drought 2015–2017. *Environmental Research Letters*, 13(12), 124010. <https://doi.org/10.1088/1748-9326/aae9f9>.
- Philippon, N., Rouault, M., Richard, Y. and Favre, A. (2012) The influence of ENSO on winter rainfall in South Africa. *International Journal of Climatology*, 32(15), 2333–2347. <https://doi.org/10.1002/joc.3403>.
- Pienaar, L. and Boonzaaier, J. (2018) *Drought Policy Brief: Western Cape Agriculture*. Cape Town: Western Cape Government, Bureau for Food and Agricultural Policy, 1–17. [http://www.bfap.co.za/wp-content/uploads/2018/08/DroughtPolicyBrief\\_2018.pdf](http://www.bfap.co.za/wp-content/uploads/2018/08/DroughtPolicyBrief_2018.pdf).
- Reason, C.J.C. (2017) *Climate of Southern Africa*. USA: Oxford University Press. 10.1093/acrefore/9780190228620.013.513.
- Reason, C.J.C. and Jagadheesha, D. (2005) Relationships between South Atlantic SST variability and atmospheric circulation over the South African region during austral winter. *Journal of Climate*, 18(16), 3339–3355. <https://doi.org/10.1175/JCLI3474.1>.
- Reason, C.J.C. and Rouault, M. (2005) Links between the Antarctic oscillation and winter rainfall over western South Africa. *Geophysical Research Letters*, 32(7), 1–4. <https://doi.org/10.1029/2005GL022419>.
- Riemann-Campe, K., Blender, R. and Fraedrich, K. (2011) Global memory analysis in observed and simulated CAPE and CIN. *International Journal of Climatology*, 31(8), 1099–1107. <https://doi.org/10.1002/joc.2148>.
- Schneider, U., Becker, A.P.F., Meyer-Christoffer, A, Rudolf, B, Ziese, M. (2011). GPCC Full Data Reanalysis Version 6.0 at 1.0°: Monthly Land-Surface Precipitation from Rain-Gauges built on GTS-based and Historic Data. DOI: [https://doi.org/10.5676/DWD\\_GPCC/FD\\_M\\_V7\\_100](https://doi.org/10.5676/DWD_GPCC/FD_M_V7_100).
- Sheridan, S.C. and Lee, C.C. (2011) The self-organizing map in synoptic climatological research. *Progress in Physical Geography: Earth and Environment*, 35(1), 109–119. <https://doi.org/10.1177/0309133310397582>.
- Shongwe, M.E., van Oldenborgh, G.J., van den Hurk, B.J.J.M., de Boer, B., Coelho, C.A.S. and van Aalst, M.K. (2009) Projected changes in mean and extreme precipitation in Africa under global warming. Part I: southern Africa. *Journal of Climate*, 22, 3819–3837. <https://doi.org/10.1175/2009JCLI2317.1>.
- Sousa PM, Blamey RC, Reason CJC, Ramos AM, Trigo RM. 2018. The ‘Day Zero’ Cape Town drought and the poleward migration of moisture corridors. *Environmental Research Letters* 13 (12): 124025. DOI: 10.1088/1748-9326/aaebc7.
- Tyson, P.D. and Preston-Whyte, R.A. (2000) *The Weather and Climate of Southern Africa*. USA: Oxford University Press.
- Vesanto, J. and Alhoniemi, E. (2000) Clustering of the self-organizing map. *IEEE Transactions on Neural Networks*, 11(3), 586–600. <https://doi.org/10.1109/72.846731>.
- Wolski, P. (2018) How severe is Cape Town’s “Day Zero” drought? *Significance*, 15(2), 24–27. <https://doi.org/10.1111/j.1740-9713.2018.01127.x>.
- Wolski, P., Jack, C., Tadross, M., van Aardenne, L. and Lennard, C. (2018) Interannual rainfall variability and SOM-based circulation classification. *Climate Dynamics*, 50(1–2), 479–492. <https://doi.org/10.1007/s00382-017-3621-1>.

## SUPPORTING INFORMATION

Additional supporting information may be found online in the Supporting Information section at the end of this article.

**How to cite this article:** Odoulami RC, Wolski P, New M. A SOM-based analysis of the drivers of the 2015–2017 Western Cape drought in South Africa. *Int J Climatol*. 2020;1–13. <https://doi.org/10.1002/joc.6785>